Surface Tension of the System $NaF–AlF_3–Al_2O_3$ and Surface Adsorption of Al_2O_3

Marián Kucharík and Roman Vasiljev

Institute of Inorganic Chemistry, Slovak Academy of Sciences, Dúbravská cesta 9, 845 36 Bratislava, Slovakia

Reprint requests to M. K.; Fax: ++421-(0)2-59410444; E-mail: uachkuch@savba.sk

Z. Naturforsch. **61a,** 389 – 398 (2006); received May 9, 2006

Part of the molten system $NaF–AlF_3–Al_2O_3$ was studied by surface tension measurements, which were performed at cryolite ratios (*CR*) between 1.5 and 3 [$CR = n(NaF)/n(AlF_3)$]. The maximal bubble pressure method was applied. The surface adsorption of alumina (Al_2O_3) was also calculated. The obtained results were discussed in terms of the anionic composition of the melt. The addition of AlF_3 to melt with $CR = 3$ decreases the surface tension, as AlF_3 is surface-active in molten Na_3AlF_6. The concentration dependence of the surface tension and the surface adsorption of alumina in the title system are influenced by the formation of surface-active oxofluoroaluminates. An increase of the difference between the surface tension of $NaF–AlF_3$ mixtures and the surface tension of pure alumina was observed with decreasing cryolite ratio.

Key words: Maximal Bubble Pressure Method; Surface Activity; Ionic Entities; Cryolite Melts; Alumina.

1. Introduction

In the production of aluminium by the Hall-Héroult process alumina (Al_2O_3) is electrolyzed in a molten $NaF–AlF_3$ mixture. The surface tension is an important parameter which affects the industrial electrolytic production of aluminium. Several interfaces are present in the aluminium electrolysis cell. The interfacial tension between the electrolyte and molten aluminium is connected with the solution rate of aluminium in the electrolyte. The interfacial tension between the carbon parts and the electrolyte affects the penetration of the electrolyte into the carbon lining. The surface tension of the molten bath influences the separation of the carbon particles from the electrolyte and the coalescence of the fine aluminium droplets [1].

Grjotheim et al. [2] pointed out that the published surface tension data till 1980 are controversial, and further investigations have to be made. In 1983 Bratland et al. [3] published new surface tension data of the molten systems cryolite (Na_3AlF_6)–Al_2O_3 and $Na_3AlF_6–CaF_2$. They used the pin detachment method for measuring the surface tension. Their results differ significantly from those published before 1980. The reasons of these differences were also given.

Fernandez et al. [4] used as Bratland et al. [3] the pin detachment method for measuring the surface tension of cryolite-based melts. Their data confirmed Bratland's results.

Fernandez and Østvold [5] measured the surface tension of different molten cryolite-based systems. In the molten system $NaF–AlF_3$ the surface tension decreases with increasing concentration of AlF_3. Evidently AlF_3 is a surface-active component in the $NaF–AlF_3$ system.

Daněk et al. [6] published surface tension data of low-temperature electrolytes containing AlF_3, LiF, KF, CaF_2 and Al_2O_3.

Surface tension data are interesting from both the technological and structural point of view. More covalent species concentrate at the surface of the melt.

The ionic structure of cryolite melts has been discussed for more than 75 years, but it is still controversial [1]. Nowadays it is generally accepted that molten Na_3AlF_6 is completely dissociated into ionic entities. In 1975 Gilbert et al. [7] did not detect any spectral evidence for AlF_3 as an entity in liquid $NaF–AlF_3$ mixtures, and hence the presence of AlF_3 was excluded in molten cryolite. They discussed the presence of AlF_6^{3-} and AlF_4^- in the molten system $NaF–AlF_3$, only. The following dissociation scheme of molten cryolite was

considered up to 1986:

$$Na_3AlF_6 = 3Na^+ + AlF_6^{3-},$$
$$AlF_6^{3-} = AlF_4^- + 2F^-.$$

In 1986 Dewing [8] modified this dissociation scheme. Based on thermodynamic modeling, applying his own activity data for NaF and AlF_3, he concluded that the AlF_5^{2-} anion should be a major entity in the molten cryolite. Dewing proposed the following dissociation reactions:

$$AlF_6^{3-} = AlF_5^{2-} + F^-,$$
$$AlF_5^{2-} = AlF_4^- + F^-.$$

Gilbert and Materne [9] reinvestigated the molten NaF–AlF_3 mixtures by Raman spectroscopy. The band at 555 cm^{-1}, previously assigned to AlF_6^{3-} [7], was now interpreted as originating from AlF_5^{2-}. A weak shoulder at 515 cm^{-1}, heavily overlapped by the 555 cm^{-1} band, was assigned to AlF_6^{3-}. On the other hand, Brooker et al. [10] performed a Raman study of an eutectic LiF–NaF–KF mixture after addition of either AlF_3 or Na_3AlF_6. The transition from the solid to the liquid state at about 455 °C occurred without change in the peak positions, half-widths and relative intensities. The bands detected in the liquid phase were thus assigned to AlF_6^{3-}. There was no evidence of a shoulder on the low frequency side of the AlF_6^{3-} band, as reported previously by Gilbert and co-workers [9, 11, 12]. Robert et al. [13] investigated the molten system NaF–AlF_3 by high-temperature ^{27}Al NMR. The experimental chemical shifts were compared to the shifts calculated on the basis of their previous Raman model [11, 12] with AlF_6^{3-}, AlF_5^{2-} and AlF_4^-.

The ionic composition of cryolite systems with alumina is more complicated. From cryoscopy measurements on the sodium fluoride-rich side in the reciprocal salt system NaF–AlF_3–Na_2O–Al_2O_3 Førland and Ratkje [14] suggested the preferred formation of $Al_2OF_x^{(4-x)}$ ($x = 5-8$) anions.

From vapour pressure measurements Kvande [15] proposed the formation of $Al_2OF_8^{4-}$ as the most important anion at low alumina content in cryolite melts.

Sterten [16] developed an ionic structure model for NaF–AlF_3 melts containing alumina. The calculation of anion fractions as functions of the cryolite ratio (*CR*) suggested $Al_2OF_6^{2-}$ and $Al_2O_2F_4^{2-}$ as the most frequent species for $1.5 < CR > 3$ [$CR = n(NaF)/n(AlF_3)$]. For $CR > 5$ the complex anions $Al_2O_2F_4^{2-}$ and $Al_2O_2F_6^{4-}$ were most important.

The Raman data and thermodynamic measurements of Gilbert et al. [12] and Robert et al. [17] indicate the formation of $Al_2OF_6^{2-}$ or $Al_2OF_8^{4-}$ in melts with low Al_2O_3 concentrations. However, $Al_2O_2F_4^{2-}$ would be predominant at higher Al_2O_3 concentration. The above assumption was confirmed by Lacassagne et al. [18]. They studied the structure of NaF–AlF_3–Al_2O_3 melts by high-temperature NMR for the four nuclei ^{27}Al, ^{23}Na, ^{19}F, ^{17}O. ^{17}O NMR gave a selective view of the alumina solution in molten cryolite because of its direct signature of the oxofluoride complexes. The variations of the ^{17}O chemical shift were explained by at least two different oxofluoroaluminate species: $Al_2OF_6^{2-}$, at low alumina content and $Al_2O_2F_4^{2-}$, that becomes the major species for higher amounts of alumina. The presence of some other oxygen containing species in the cryolite-alumina-based systems is still an open question. A detailed literature review on possible ionic entities in cryolite melts with or without alumina is presented in [19].

In the present work the surface tension of the ternary system NaF–AlF_3–Al_2O_3 is studied and the surface adsorption of alumina is calculated. The obtained results are discussed in terms of the anionic composition.

2. Experimental

2.1. Apparatus

Figure 1 shows the apparatus for the measurement of the surface tension with the maximal bubble pressure method. The measuring device consisted of a resistance furnace with a special water-cooled furnace lid with an adjustable head fixing the position of a PtRh20 capillary, a working Pt/PtRh10 thermocouple and a platinum wire. The platinum wire served as electrical contact to adjust the exact touch of the capillary with the molten salt surface. A micrometer screw, fixed on the lid, moved the head and determined the exact position for the touch of the capillary with the liquid surface. It enabled to define the required depth of immersion with an accuracy of ± 0.01 mm. A PtRh20 capillary with an outer diameter of 3 mm was used. In order to obtain precise results, the capillary tip was carefully machined. The orifice had to be as circular as possible, with a sharp conical edge. A precise inner diameter of the capillary is very important for accurate measurements.

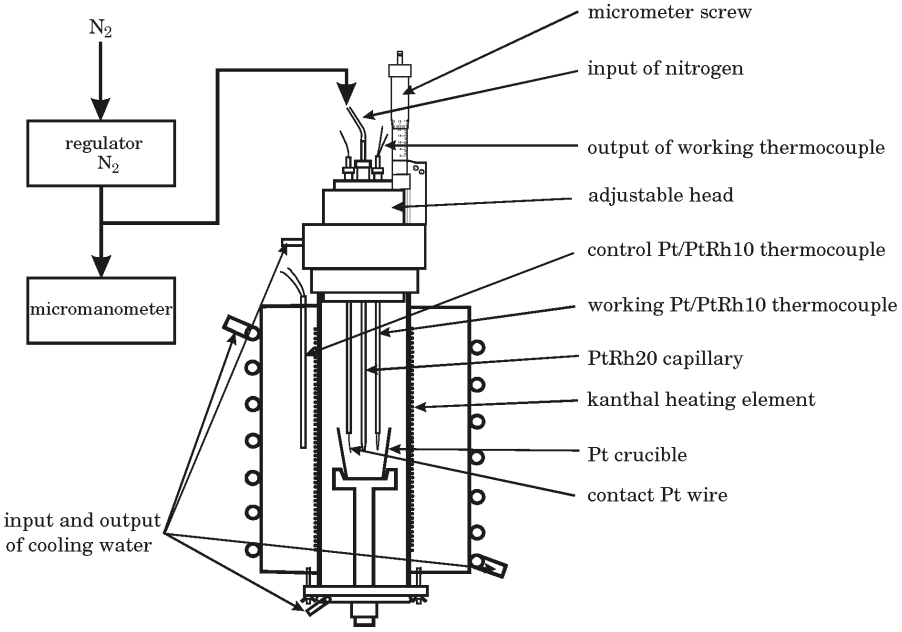

Fig. 1. Apparatus for measurement of the surface tension of molten salts with the maximal bubble pressure method.

The inner diameter of the capillary at room temperature was calculated from measured surface tensions of water and acetone, the values which are well established. The equation for the thermal expansion of the PtRh20 alloy was used for the calculation of the actual capillary diameter at the measuring temperature.

An additional Pt/PtRh10 control thermocouple, placed very close to the heating shaft of the furnace, was connected with the temperature controller Micromega ICN 77343C2 to adjust the required working temperature. The working Pt/PtRh10 thermocouple, placed at the furnace, was calibrated by the known melting points of NaCl, KCl and NaF. The voltameter MT-100, calibrated with the very precise multimeter KEITHLEY 2700, was used for the temperature measurements.

The digital micromanometer COMMET LB/ST 1000 with two measuring ranges, 200 Pa and 1000 Pa, was used for the pressure determination. This enabled us to measure the pressure with an accuracy of ± 1 Pa. Nitrogen, conducted through concentrated sulphuric acid in order to remove water traces, was used to form the bubbles and to maintain an inert atmosphere above the sample. When the capillary was above the melt between the measurements, the inert gas was slowly fed through the capillary to avoid condensation in the upper part of the capillary. During the measurements the rate of bubble formation was approximately 1 bubble per 15 – 25 s.

2.2. Procedure

The surface tension can be calculated according to [20] by

$$\gamma = \frac{r}{2}(p_{\max} - gh\rho), \tag{1}$$

where r is the capillary radius, $p_{\max}$ the maximal bubble pressure when the bubble is a hemisphere with the radius equal to the radius of the capillary, g is the gravitational constant, h the depth of immersion of the capillary and ρ the density of the melt. It should be noted that in reality cavities are formed, not bubbles. Solheim [21] published an empirical equation for the density of the molten system NaF–LiF–AlF_3–CaF_2–Al_2O_3. Solheim's equation is based on the experimental data cited in a monograph of Thonstad et al. [1] and reliable density data that are summarized in a monograph of Grjotheim et al. [2].

However, there is also a possibility of calculating the surface tension of the liquid without knowing the density of the melt. In the present case the density ρ of the melt can be eliminated from (1), and for two different immersion depths the following equation is valid:

$$\gamma = \frac{r}{2}\frac{p_{\max,1}h_2 - p_{\max,2}h_1}{h_2 - h_1}, \tag{2}$$

where $p_{\max,i}$ is the maximal bubble pressure at the immersion depth h_i ($h_1 < h_2$).

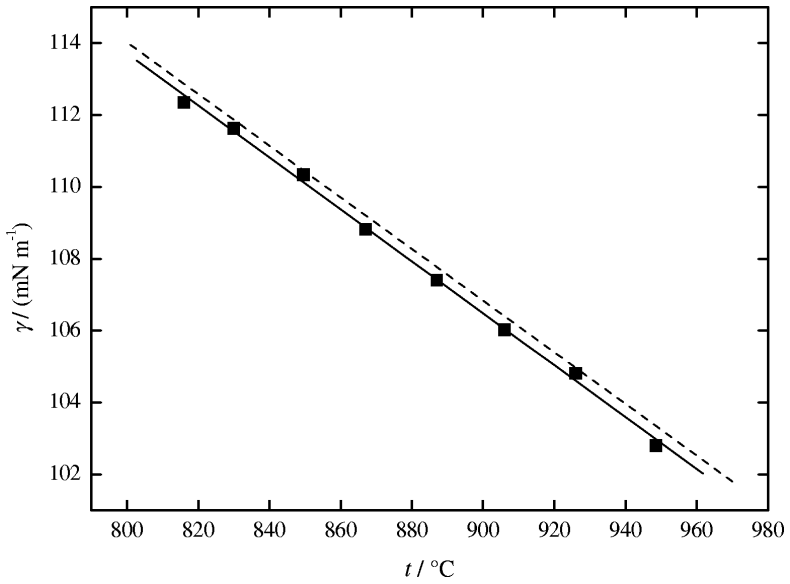

Fig. 2. Surface tension of molten NaCl. ■, This work; ---, Janz et al. [24].

In the present study (2) was used, where an error from the density determination is overcome.

The surface tension of each sample was measured at 5 – 7 different temperatures in the range of 80 – 120 °C, starting at approximately 20 °C above the temperature of primary crystallization, t_{pc}, which was obtained from the literature [22].

Because of an increase in the total vapour pressure above the melts with a higher amount of aluminium fluoride, the time of melting those mixture (especially at $CR = 1.5$) was shortened.

By measuring the selected mixtures repeatedly it was shown that no significant change in the surface tension did occur.

The measurements were made at four depths of immersion (2, 3, 4 and 5 mm), yielding six surface tension values for each temperature.

2.3. Precision and Accuracy

The estimated experimental accuracy of the maximal bubble pressure method is ca. ±1% [23]. Molten sodium chloride was used as reference to determine the accuracy of the measurements. The obtained data are compared in Fig. 2 with recommended data given by Janz et al. [24].

The maximum deviation between the recommended and the presented data was 0.5%.

2.4. Chemicals

Natural hand-picked Na_3AlF_6 was from Greenland (melting point: 1009 – 1011 °C), AlF_3 sublimated under vacuum in a graphite crucible, AlF_3 sublimated in a platinum crucible, Al_2O_3 (p. a.) from Merck, and NaCl, KCl and NaF were all from Fluka (p. a.). All chemicals were dried for several hours at 500 °C before use. N_2 (99.90%) was conducted through concentrated sulphuric acid in order to remove traces of water.

3. Results and Discussion

Fernandez and Østvold [5] reported that their frozen melt containing AlF_3, sublimated in a graphite crucible, displayed a surface of greyish colour, and the reproducibility of the surface tension measured in this melt was bad. The reason of this behaviour was probably the presence of small carbon particles from the graphite crucible. These carbon particles float on the melt and concentrate on the surface. In the present case good agreement was observed between the surface tension data of natural hand-picked Na_3AlF_6 from Greenland, synthetic Na_3AlF_6 (AlF_3 sublimated in a graphite crucible and AlF_3 sublimated in a platinum crucible, respectively) and the most reliable previously reported data [3, 5] (Fig. 3). The maximum deviation was 0.7%. This is still within the limits of accuracy of the maximal bubble pressure method. The use of AlF_3 sublimate in a graphite crucible exhibited no influence on

x_{NaF}	x_{AlF_3}	$x_{Al_2O_3}$	a (mN m^{-1})	b (mN m^{-1} °C^{-1})	SD (mN m^{-1})	t (°C)
0.7500	0.2500	0.0000	274.61	0.1383	0.29	1020 – 1125
0.7382	0.2461	0.0157	242.85	0.1127	0.26	1025 – 1119
0.7220	0.2407	0.0373	226.35	0.0974	0.38	1017 – 1112
0.7091	0.2364	0.0545	239.57	0.1104	0.24	987 – 1103
0.7091	0.2364	0.0545	229.57	0.1005	0.35	998 – 1092
0.6964	0.2321	0.0714	226.30	0.0972	0.14	1045 – 1139
0.7138	0.2862	0.0000	272.49	0.1476	0.26	1029 – 1121
0.7138	0.2862	0.0000	259.23	0.1342	0.27	1018 – 1110
0.7023	0.2816	0.0161	248.04	0.1259	0.39	1009 – 1092
0.6865	0.2752	0.0383	223.16	0.1027	0.32	1010 – 1101
0.6767	0.2713	0.0520	220.18	0.0992	0.27	999 – 1092
0.6657	0.2669	0.0674	212.88	0.0926	0.20	1036 – 1129
0.6670	0.3330	0.0000	242.57	0.1344	0.39	981 – 1074
0.6596	0.3293	0.0111	227.24	0.1212	0.05	960 – 1033
0.6596	0.3293	0.0111	231.36	0.1248	0.21	969 – 1045
0.6559	0.3274	0.0167	237.29	0.1323	0.32	971 – 1040
0.6483	0.3236	0.0281	212.95	0.1081	0.21	970 – 1039
0.6392	0.3191	0.0417	210.60	0.1037	0.37	962 – 1037
0.6327	0.3158	0.0515	227.58	0.1190	0.65	988 – 1082
0.6000	0.4000	0.0000	189.78	0.1142	0.21	855 – 936
0.5965	0.3977	0.0058	218.73	0.1449	0.24	833 – 925
0.5913	0.3942	0.0146	184.84	0.1055	0.34	833 – 912
0.5869	0.3913	0.0218	178.93	0.0989	0.20	822 – 885
0.5823	0.3882	0.0294	189.09	0.108	0.33	900 – 990
0.5787	0.3858	0.0355	187.5	0.103	0.44	952 – 1008

Table 1. Coefficients a and b in (3), standard deviations (SD) and the temperature range of the measurements.

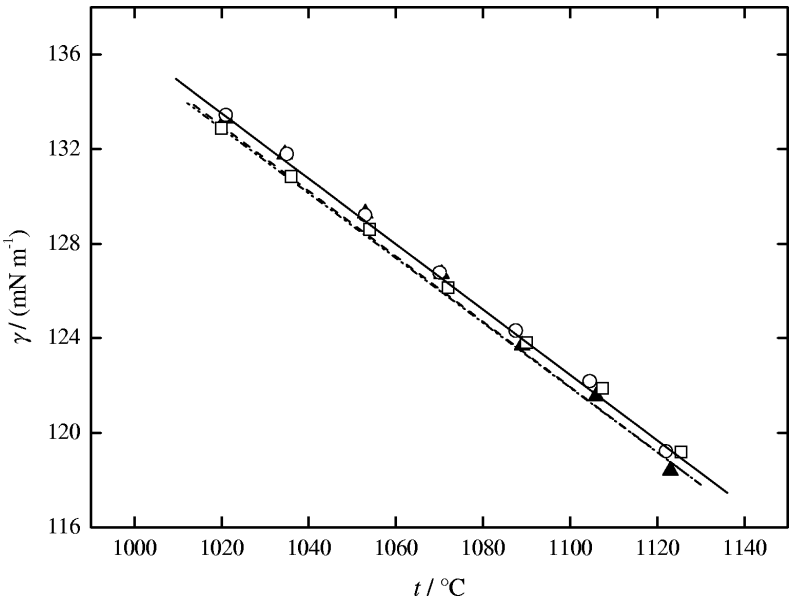

Fig. 3. Temperature dependence of the surface tension of pure cryolite. ▲, This work: natural hand-picked Na_3AlF_6 from Greenland; ○, this work: synthetic Na_3AlF_6, AlF_3 sublimated in a platinum crucible; □, this work: synthetic Na_3AlF_6, AlF_3 sublimated in a graphite crucible; · – ·, Bratland et al. [3]; ---, Fernandez and Østvold [5].

the surface tension, and the reproducibility was good, as well. The frozen melt showed a white colour in the whole volume and on the surface. The quality of the used carbon as material for the crucible has a major influence on the quality of the produced AlF_3.

In a restricted temperature range the experimental temperature dependence of the surface tension can be expressed by the linear equation

$$\gamma = a - bt, \tag{3}$$

where γ is the surface tension in mN m^{-1} and t is the temperature in °C.

The melt compositions and the values of the constants a and b in (3), obtained from the linear re-

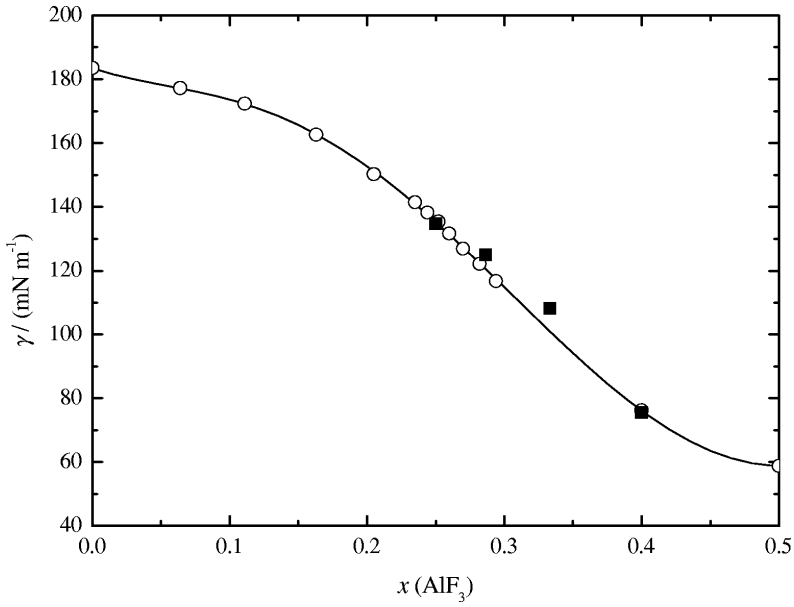

Fig. 4. Surface tension of NaF–AlF_3 mixtures. ○ and line, Fernandez and Østvold [5]; ■, this work; $t = 1000$ °C.

Table 2. Coefficients A_j and the standard deviation (*SD*) in (4) for three selected temperatures.

A_j(mN m^{-1})	Temperature		
	975 °C	1000 °C	1025 °C
A_1	68 ± 15	72 ± 18	76 ± 22
A_2	-17285 ± 2551	-16486 ± 2964	-15741 ± 3571
A_3	16186 ± 2523	15404 ± 2931	14675 ± 3531
A_4	18275 ± 2605	17427 ± 3026	16635 ± 3645
A_5	1246 ± 232	1172 ± 270	1102 ± 325
A_6	9170 ± 1190	8824 ± 1381	8506 ± 1664
SD	0.9	1.0	1.2

gression analysis, together with the values of the standard deviation of approximation are given in Table 1. The selected compositions cover the region of the system NaF–AlF_3–Al_2O_3 which is interesting for the industrial aluminium electrolysis. The measurements were carried out at four cryolite ratios [$CR = n(\mathrm{NaF})/n(\mathrm{AlF_3})$], 3, 2.5, 2 and 1.5.

The following final equation describing the dependence of the surface tension on the composition was obtained:

$$\begin{aligned}\gamma/(\mathrm{mN\,m^{-1}}) &= A_1 x_{\mathrm{NaF}} \\ &+ x_{\mathrm{NaF}} x_{\mathrm{AlF_3}} (A_2 + A_3 x_{\mathrm{AlF_3}} + A_4 x_{\mathrm{NaF}}) \\ &+ A_5 x_{\mathrm{NaF}} x_{\mathrm{Al_2O_3}} + A_6 x_{\mathrm{AlF_3}} x_{\mathrm{Al_2O_3}} .\end{aligned} \tag{4}$$

The calculation of the coefficients A_j in (4) was performed using multiple linear regression analysis, omitting the statistically nonimportant terms on the 0.95 confidence level.

The calculated values of the coefficients A_j and the standard deviations of the approximation for three chosen temperatures (975 °C, 1000 °C and 1025 °C) are given in Table 2.

The surface tension of the system NaF–AlF_3 at 1000 °C is presented in Figure 4.

The surface tension of molten sodium fluoride decreases with increasing amount of aluminium fluoride. This implies that AlF_3 is a surface-active component in the system NaF–AlF_3. This behavior was explained by the formation of AlF_6^{3-}, AlF_5^{2-} and AlF_4^- complex anions [8, 9, 11, 12]. They will concentrate on the surface of the melt, reducing the surface tension. A more detailed explanation of the influence of ionic species on the surface tension of cryolite-based melts was published in [5, 23].

The dependences of the surface tension on the content of alumina at four cryolite ratios *CR* are shown in Figure 5.

At $CR = 3$ the surface tension decreases at low alumina contents [up to $x(\mathrm{Al_2O_3}) \approx 0.04$], and then the surface tension reaches a constant value with further increasing of alumina content. Identical results in the investigated concentration range were observed by Bratland et al. [3] and Fernandez et al. [4]. A similar behaviour of the surface tension is observed at $CR = 2.5$, however with lower surface tension values than at $CR = 3$ (Fig. 5). The surface tension at $CR = 2$ decreases, reaches a minimum and then in-

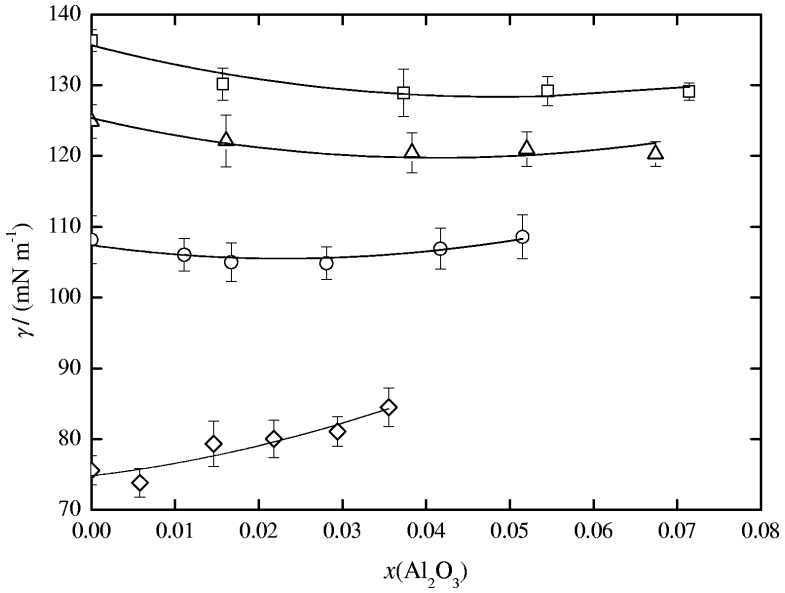

Fig. 5. Surface tension of molten NaF–AlF_3–Al_2O_3 at four cryolite ratios. □, $CR = 3$; △, $CR = 2.5$; ○, $CR = 2$; ◇, $CR = 1.5$; lines, equation (2); t = 1000 °C.

creases with further alumina addition. The surface tension at $CR = 1.5$ is increasing with increasing alumina content.

The surface adsorption of alumina was calculated for all four cryolite ratios at 1000 °C in the following way.

Gibbs' equation for the surface tension is obtained by converting the equation for Gibbs' energy of a liquid surface at constant pressure, and it is in general valid for the surfaces of molten systems [25]:

$$\mathrm{d}\gamma = -s^{\mathrm{s}}\mathrm{d}T - \sum_i \Gamma_i \mathrm{d}\mu_i^{\mathrm{s}}, \tag{5}$$

where γ is the surface tension, s^{s} the surface entropy per unit area, Γ_i the surface adsorption and μ_i^{s} the chemical potential of the component i in the surface layer.

At equilibrium the chemical potentials of all components in the surface phase have to be equal to the chemical potentials in the bulk liquid and in the gas phase. Therefore the chemical potentials μ_i^{s} in the surface phase can be replaced by the chemical potentials in the bulk liquid μ_i.

At constant temperature, for the molten system NaF–AlF_3–Al_2O_3 one can write

$$\mathrm{d}\gamma = -\Gamma_1 \mathrm{d}\mu_1 - \Gamma_2 \mathrm{d}\mu_2 - \Gamma_3 \mathrm{d}\mu_3. \tag{6}$$

In the further text the meaning of the indexes is as follows:

$$1 = \mathrm{NaF}, \quad 2 = \mathrm{AlF_3}, \quad 3 = \mathrm{Al_2O_3}.$$

Provided that $\Gamma_1 \approx \Gamma_2 \approx 0$ is chosen, this gives

$$-\Gamma_3 = \left(\frac{\mathrm{d}\gamma}{\mathrm{d}\mu_3}\right)_{T,p}. \tag{7}$$

This simplification of Gibbs' equation in the ternary system NaF–AlF_3–Al_2O_3 can be used only in cross-sections with a constant ratio of the amounts of selected substances. In the system NaF–AlF_3–Al_2O_3 the pseudo-binary systems NaF/AlF_3–Al_2O_3 were chosen.

For the derivative of the experimentally determined concentration dependence $\gamma = \mathrm{f}(x_3)$ of the surface tension of the pseudo-binary systems NaF/AlF_3–Al_2O_3 it can be written as [25]:

$$\left(\frac{\mathrm{d}\gamma}{\mathrm{d}x_3}\right)_{T,p} = \left(\frac{\mathrm{d}\gamma}{\mathrm{d}\mu_3}\right)_{T,p} \left(\frac{\mathrm{d}\mu_3}{\mathrm{d}x_3}\right)_{T,p}. \tag{8}$$

For the chemical potential of alumina in the liquid phase it can be written:

$$\mu_3 = \mu_3^0 + RT \ln a_3. \tag{9}$$

Differentiating (9) we get

$$\left(\frac{\mathrm{d}\mu_3}{\mathrm{d}x_3}\right)_{T,p} = RT \left(\frac{\mathrm{d}\ln a_3}{\mathrm{d}x_3}\right)_{T,p}, \tag{10}$$

and inserting (7) and (10) into (8) it follows:

$$\left(\frac{\mathrm{d}\gamma}{\mathrm{d}x_3}\right)_{T,p} = -\Gamma_3 RT \left(\frac{\mathrm{d}\ln a_3}{\mathrm{d}x_3}\right)_{T,p}. \tag{11}$$

Table 3. Compositions (x_i), values of terms in (12), and calculated surface adsorption of alumina; $t = 1000$ °C.

x_{NaF}	x_{AlF_3}	$x_{Al_2O_3}$	$\left(\frac{d\ln a_{Al_2O_3}}{dx_{Al_2O_3}}\right)_{T,p}$	$\left(\frac{d\gamma}{dx_{Al_2O_3}}\right)_{T,p}$	$\Gamma_{Al_2O_3}(10^{-5}\ \mathrm{mol\,m^{-2}})$
0.7500	0.2500	0.0000	∞	−886.1575	0
0.7382	0.2461	0.0157	130.2238	−130.7756	9.4890
0.7220	0.2407	0.0373	42.9375	−9.3237	2.0520
0.7091	0.2364	0.0545	26.3802	−1.1401	0.4084
0.7091	0.2364	0.0545	26.3802	−1.1401	0.4084
0.6964	0.2321	0.0714	18.7365	−0.1446	0.0729
0.7138	0.2862	0.0000	∞	−285.6590	0
0.7023	0.2816	0.0161	126.6269	−104.9116	7.8280
0.6865	0.2752	0.0383	42.0000	−26.3660	5.9310
0.6767	0.2713	0.0520	28.4823	−11.2972	3.7480
0.6657	0.2669	0.0674	20.5368	−4.3419	1.9980
0.6670	0.3330	0.0000	∞	−270.8598	0
0.6596	0.3293	0.0111	203.2173	−144.7572	6.7300
0.6596	0.3293	0.0111	203.2173	−144.7572	6.7300
0.6559	0.3274	0.0167	122.9075	−83.1062	6.3890
0.6483	0.3236	0.0281	63.9176	37.2252	−5.5030
0.6392	0.3191	0.0417	38.7499	172.7735	−42.130
0.6327	0.3158	0.0515	29.6926	264.9874	−84.320
0.6000	0.4000	0.0000	∞	183.4084	0
0.5965	0.3977	0.0058	445.6742	210.0901	−4.4540
0.5913	0.3942	0.0146	152.6881	250.5408	−15.500
0.5869	0.3913	0.0218	93.9991	283.7983	−28.530
0.5823	0.3882	0.0294	65.1382	319.1253	−46.290
0.5787	0.3858	0.0355	51.9028	346.9763	−63.160

Finally a common equation for the surface adsorption of alumina in the pseudo-binary molten systems NaF/AlF_3–Al_2O_3 can be derived:

$$\Gamma_3 = -\frac{1}{RT}\frac{\left(\frac{d\gamma}{dx_3}\right)_{T,p}}{\left(\frac{d\ln a_3}{dx_3}\right)_{T,p}}. \qquad (12)$$

At equilibrium, the chemical potential of alumina in the surface phase has to be equal to the chemical potential of alumina in the bulk liquid, as stated above. Therefore the empiric equations for the activity of alumina in the molten system NaF–AlF_3–Al_2O_3, derived by Solheim and Sterten [26], can be used for the calculation of the term $(d\ln a_3/dx_3)_{T,p}$:

$$\ln a_{3(T)} = \ln a_{3(1300)} + \frac{\bar{H}_3}{R}\left(\frac{1}{T} - \frac{1}{1300}\right), \qquad (13a)$$

where

$$\ln a_{3(1300)} = 3\ln x_3 - \frac{103.1 + 3.3CR - 1.7(3-CR)^5}{54}\ln(1+54x_3) + 11.16 \qquad (13b)$$

and

$$\bar{H}_3 = 87 + 0.7875(CR-1)^2[1 + (59-60x_3)\mathrm{e}^{-60x_3}], \qquad (13c)$$

where CR is the cryolite ratio and $\bar{H}_3$ is the partial enthalpy of mixing for Al_2O_3 in $\mathrm{kJ\,mol^{-1}}$. The derived empiric equations are consistent with the Gibbs-Duhem equation. These equations show good agreement with the experimental data available in the literature, such as heat of dissolution, liquidus temperature, alumina solubility, vapour pressure and EMF of electrochemical concentration cells.

After inserting (13b) and (13c) into (13a) and consequent derivation with respect to x_3 we obtain the final equation for the term $(d\ln a_3/dx_3)_{T,p}$:

$$\left(\frac{d\ln a_3}{dx_3}\right)_{T,p} = \frac{3}{x_3} - \frac{103.1 + 3.3CR - 1.7(3-CR)^5}{1+54x_3} + \frac{2835(CR-1)^2(x_3-1)\cdot\mathrm{e}^{-60x_3}}{R}\left(\frac{1}{T} - \frac{1}{1300}\right), \qquad (14)$$

which was used for the calculation of the surface adsorption of alumina according to (12).

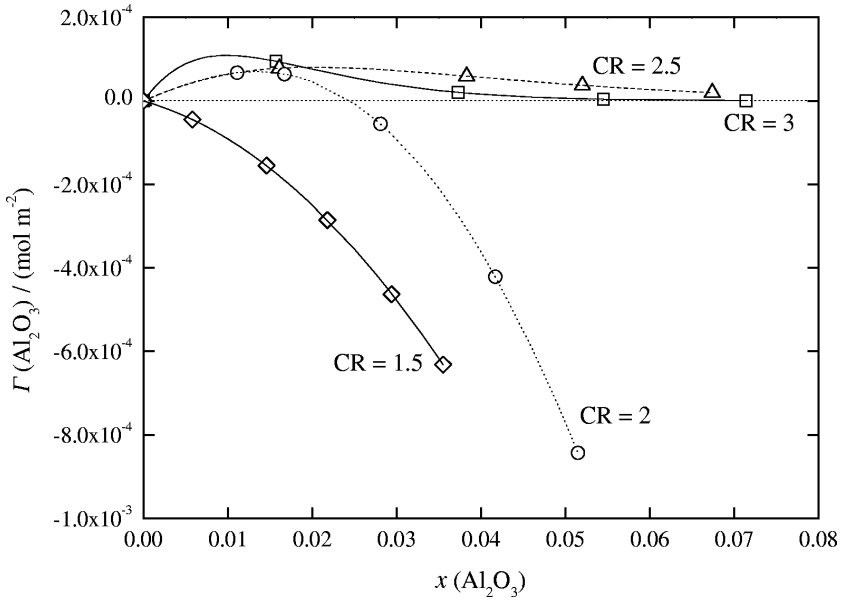

Fig. 6. Surface adsorption of alumina in molten NaF–AlF_3–Al_2O_3 at four cryolite ratios *CR*; $t = 1000$ °C.

The values of terms of (12) and the surface adsorption of alumina calculated by this equation at 1000 °C are given in Table 3.

The surface adsorption is positive when the term $(\mathrm{d}\gamma/\mathrm{d}x_{\mathrm{Al_2O_3}})_{T,p}$ is negative and vice versa. In general, when the surface tension decreases, the added compound (solvent compound) will be surface-active and concentrated on the surface, and the surface adsorption will be positive. The dependences of the surface adsorption of alumina on the alumina content and cryolite ratio are presented in Figure 6.

It is obvious that the surface tension is influenced by the presence of ionic constituents in the melt. Ionic constituents of the investigated melts come from different processes: (i) melting; (ii) dissociation; (iii) dissolution and (iv) mutual reaction. Consequently, the investigated melt will consist of a relatively large number of different ionic species. However the concentration profile of each ionic component is unknown, as the system is too complex, and moreover, the presence of some ionic species is still under discussion. Based on the most accepted studies, the following explanation of the observed surface tension can be suggested.

As it was mentioned above, different authors suggested that $Al_2OF_6^{2-}$, $Al_2OF_8^{4-}$and $Al_2O_2F_4^{2-}$ are the most frequent oxofluoroaluminate species for $1.5 < CR < 3$. It is expected that these complex anions will be concentrated in the surface, reducing the surface tension. Approximately similar values of the surface adsorption of alumina [$x(Al_2O_3) \approx 0.017$] are observed at cryolite ratios equal to 3, 2.5 and 2. At these compositions, the presence of $Al_2OF_6^{2-}$ and $Al_2OF_8^{4-}$ anions is expected at the lower alumina concentrations [12, 15 – 18, 27]. These anions are thus probably responsible for the decrease of the surface tension (positive values of the surface adsorption of alumina). Further addition of alumina would result in the appearance of $Al_2O_2F_4^{2-}$ resulting in a slight increase of the surface tension for $CR = 3$ and 2.5, and a more pronounce increase at $CR = 2$. The surface adsorption of alumina at $CR = 2$ after reaching the maximum begins to decrease to negative values. As at $CR = 1.5$ the system is rich in aluminium, the formation of the first two anions is suppressed and only $Al_2O_2F_4^{2-}$ is present, leading to an increase in the surface tension.

Symmetry is an important factor that should be considered for the explanation of surface properties of melts. The higher the local symmetry the higher the energy which is needed for reorientation of the surface layers. Consequently, constituents that lower the local symmetry of the melt will lower the surface tension and vice versa. Thus the anions $Al_2OF_6^{2-}$ and $Al_2OF_8^{4-}$, which lower the symmetry, may be considered as agents lowering the surface tension, and the anion $Al_2O_2F_4^{2-}$, having higher symmetry, as agent increasing the surface tension. This corresponds to the observed behaviour of the surface tension of the investigated system at $CR = 1.5$ (paragraph above).

To the factors affecting the surface tension in mixtures belongs the difference between the surface tensions of pure components. The surface tension of pure Al_2O_3 near the melting point (ca. 2050 °C) is $(606 \pm 6$ mN m^{-1} [28]. The surface tension of alumina at the present measuring temperatures will probably be much higher than that of cryolite-based melts. Therefore only an increase in the surface tension at the high alumina concentrations of cryolite ratios equal to 3, 2.5 and 2 is expected. Because of the difference between surface tensions of the NaF–AlF_3 melt at $CR = 1.5$ and alumina is higher than the difference between surface tensions of NaF–AlF_3 melts at $CR = 3$, 2.5 and 2, only an increase of the surface tension with increasing concentration of alumina was observed.

4. Conclusion

The following trends have been found for the surface tension of the investigated system: (i) the surface tension of melts free of alumina decreases with decreasing cryolite ratio; (ii) the surface tension decreases with initial alumina addition followed by a slight increase at $CR = 3$, 2.5 and 2; (iii) at $CR = 1.5$ the surface tension increases only with increasing alumina content. Based on the most accepted literature data, the anions $Al_2OF_6^{2-}$ and $Al_2OF_8^{4-}$ are assumed to be the surface-active species.

Acknowledgements

The Slovak Grant Agencies (VEGA-2/4071/04, APVT-51-008104) are acknowledged for financial support.

[1] J. Thonstad, P. Fellner, G. M. Haarberg, J. Híveš, H. Kvande, and Å. Sterten, Aluminium Electrolysis. Fundamentals of the Hall-Héroult Process, 3rd ed., Aluminium-Verlag, Düsseldorf, Germany 2001.
[2] K. Grjotheim, C. Krohn, M. Malinovský, K. Matiašovský, and J. Thonstad, Aluminium Electrolysis. Fundamentals of the Hall-Héroult Process, 2nd ed., Aluminium Verlag, Düsseldorf, Germany 1982.
[3] D. Bratland, C. M. Ferro, and T. Østvold, Acta Chem. Scand. **37A**, 487 (1983).
[4] R. Fernandez, K. Grjotheim, and T. Østvold, Light Met., 1025 (1986).
[5] R. Fernandez and T. Østvold, Acta. Chem. Scand. **43**, 151 (1989).
[6] V. Daněk, O. Patarák, and T. Østvold, Can. Metall. Qu. **34**, 129 (1995).
[7] B. Gilbert, G. Mamantov, and G. M. Begun, J. Chem. Phys. **62**, 950 (1975).
[8] E. W. Dewing, Proceedings of the 5th International Symposium on Molten Salts, The Electrochemical Society Inc., Pennington, NJ 1986, pp. 262 – 274.
[9] B. Gilbert and T. Materne, Appl. Spectrosc. **44**, 299 (1990).
[10] M. H. Brooker, R. W. Berg, J. H. von Barner, and N. J. Bjerrum, Inorg. Chem. **39**, 3682 (2000).
[11] E. Tixhon, E. Robert, and B. Gilbert, Appl. Spectrosc. **48**, 1477 (1993).
[12] B. Gilbert, E. Robert, E. Tixhon, J. E. Olsen, and T. Østvold, Light Met., 181 (1995).
[13] E. Robert, V. Lacassagne, C. Bessada, D. Massiot, B. Gilbert, and J. P. Coutures, Inorg. Chem. **38**, 214 (1999).
[14] T. Førland and S. K. Ratkje, Acta Chem. Scand. **27**, 1883 (1973).
[15] H. Kvande, Electrochim. Acta **25**, 273 (1980).
[16] Å. Sterten, Electrochim. Acta **25**, 1673 (1980).
[17] E. Robert, J. E. Olsen, V. Daněk, E. Tixhon, T. Østvold, and B. Gilbert, J. Phys. Chem. B **101**, 9447 (1997).
[18] V. Lacassagne, C. Bessada, P. Florian, S. Bouvet, B. Ollivier, J. P. Coutures, and D. Massiot, J. Phys. Chem. B **106**, 1862 (2002).
[19] M. Kucharík, Thesis, Institute of Inorganic Chemistry SAS, Bratislava, Slovakia 2005.
[20] A. W. Adamson, Physical Chemistry of Surfaces, Wiley, New York 1960.
[21] A. Solheim, Aluminium Trans. **2**, 162 (2000).
[22] A. Solheim, S. Rolseth, E. Skybakmoen, L. Støen, Å. Sterten, and T. Støre, Light Met., 451 (1995).
[23] V. Daněk and T. Østvold, Acta. Chem. Scand. **49**, 411 (1995).
[24] G. J. Janz, C. B. Allen, N. P. Bansal, R. M. Murphy, and R. P. T. Tomkins, Physical Properties Data Compilations Relevant to Energy Storage. II. Molten Salts: Data on Single and Multi-Component Salts Systems, NSRDS-NBS 61, Part II, National Bureau of Standards, Washington, DC 1979.
[25] V. Daněk and I. Proks, Molten Salt Forum, Vols. 5, 6, Molten Salt Chemistry and Technology 5, Trans Tech Publications, Zürich, Switzerland 1998, pp. 205 – 212.
[26] A. Solheim and Å. Sterten, Light Met., 445 (1999).
[27] V. Daněk, Ø. T. Gustavsen, and T. Østvold, Can. Metall. Qu. **39**, 153 (2000).
[28] N. Ikemiya, J. Umemoto, S. Hara, and K. Ogino, ISIJ International **33**, 156 (1993).